Forum Comment

https://doi.org/10.1130/G46761C.1

High curvatures drive river meandering

A.Finotello[1]*, A. D'Alpaos[1], E.D. Lazarus[2], and S. Lanzoni[3]
[1]Dipartimento di Geoscienze, Università di Padova, 35131 Padua, Italy
[2]School of Geography & Environmental Science, University of Southampton, Southampton SO17 1BJ, UK
[3]Dipartimento di Ingegneria Civile, Edile e Ambientale (ICEA), Università di Padova, 35131 Padua, Italy
*E-mail: alvise.finotello@unipd.it

Sylvester et al. (2019) challenge the concept in fluvial geomorphology that meander migration rates (ζ) tend to decrease in bends of high curvature ($\mathcal{C}$) beyond a critical threshold $\mathcal{C}^* = \mathcal{C}W > 0.25$–$0.5$, where W represents the width of the river (Hooke, 2013). Analyzing several meandering rivers in the Amazon basin, and accounting for the spatial lag ($\Delta_{\mathcal{C}\zeta}$) between the respective maxima in migration rate and curvature within meander bends, Sylvester et al. find significant correlation between field data and modeled migration rates computed in two different ways—as a function of the local channel curvature, and as the weighted aggregate of the upstream curvature—suggesting a monotonic relationship between migration rates and curvature that is not limited by a critical threshold in channel curvature, as previously thought. Here, we use the authors' published data for rivers in the Amazon Basin (GSA Data Repository item 2019095) to offer that Sylvester et al. do not necessarily overturn the paradigm that migration rates reduce at high-curvature bends.

To align our analysis with the approach by Sylvester et al., we compute meander migration rates with a dynamic time-warping algorithm (https://github.com/mlt/QGIS-Processing-tools) corrected by the average spatial lag between maxima in migration rate and curvature ($\overline{\Delta_{\mathcal{C}\zeta}}$) in each individual channel reach. We show that the median binned values of migration rates ($\zeta^* = \zeta/W$) consistently plateau at width-adjusted curvatures $\mathcal{C}^* > 0.25$–0.30 in all cases except the Jutaí River (Fig. 1), suggesting saturation of ζ^* beyond a critical curvature threshold. The reaches Mamoré, Purus, and Purus2 even show a subtle decrease of ζ^* beyond $\mathcal{C}^* = 0.25$–0.50, indicating a peak in ζ^* over this critical range of $\mathcal{C}^*$. This peak in ζ^*, however, is typically observed from the maximum values of the ζ^* distribution in $\{\mathcal{C}^*; \zeta^*\}$ space, rather than the distribution's central tendency (see Hooke, 2013, and references therein). Analysis of the 95th percentiles of the ζ^* distribution reinforces evidence that bends where $\mathcal{C}^* = 0.25$–0.50 also reflect the highest ζ^*, even with the spatial lag factored in (Fig. 1).

Realistic meandering patterns arise from fluvial models in which, much as Sylvester et al. describe, channel migration rate is a function of the weighted aggregate of local and non-local curvature, and the curvature-migration lag ($\Delta_{\mathcal{C}\zeta}$) is implicitly embedded in the phase-lag between channel curvature and near-bank excess velocity, to which migration rates hold a direct proportionality (e.g., Frascati and Lanzoni, 2009). However, the morphologic characteristics of these simulated patterns show statistically meaningful deviations from natural meandering planforms (Frascati and Lanzoni, 2009). These differences are mostly related to the presence of sharp bends, where linearization of the flow field—a typical step in theoretical models—overlooks highly nonlinear processes such as the saturation of centrifugally driven secondary flow, enhanced secondary outer-bank cells, and flow separation at the outer bank (Blanckaert, 2011; Hooke, 2013). These higher-order flow dynamics contribute to mitigate bank erosion as width-adjusted curvature ($\mathcal{C}^*$) increases, adding to the nonlinear effects embedded in the integro-diferential equation governing the evolution of river bends (Seminara, 2006). As a result, this would reduce the proportionality between ζ^* and $\mathcal{C}^*$ in the way we illustrate (Fig. 1).

Moreover, the scatter obscuring a clear monotonic relationship between ζ^* and $\mathcal{C}^*$ (Fig. 1) suggests the influence of other in-channel controls on meander morphodynamics, such as the erodibility of channel banks (Hooke, 2013). Although Sylvester et al. discuss the potential for bedrock substrate to reduce migration rates, erodibility also changes with riparian vegetation, and with heterogeneous floodplain sedimentology, including fine-grained deposits sequestered in relict channel traces (Güneralp and Rhoads, 2011). Differential effects of erodibility on migration rate are particularly important in sharp bends, where highly erosion-resistant banks can compound the energy expenditure from flow separation caused by high (>80–90°) angles of incidence between the flow and the outer bank.

A more clear monotonic relationship between ζ^* and $\mathcal{C}^*$ like the one Sylvester et al. describe may emerge where reach-averaged migration rates (ζ^*_{avg}) are relatively low (Fig. 1). This suggests that heterogeneous floodplain sedimentology may exert more influence on meander dynamics (e.g., Güneralp and Rhoads, 2011) in rivers where migration rates are high, with greater autogenic capacity to modify their own floodplains.

REFERENCES CITED

Blanckaert, K., 2011, Hydrodynamic processes in sharp meander bends and their morphological implications: Journal of Geophysical Research: Earth Surface, v. 116, p. 1–22, https://doi.org/10.1029/2010JF001806.

Frascati, A., and Lanzoni, S., 2009, Morphodynamic regime and long-term evolution of meandering rivers: Journal of Geophysical Research: Earth Surface, v. 114, p. 1–12, https://doi.org/10.1029/2008JF001101.

Güneralp, I., and Rhoads, B.L., 2011, Influence of floodplain erosional heterogeneity on planform complexity of meandering rivers: Geophysical Research Letters, v. 38, L14401, https://doi.org/10.1029/2011GL048134.

Hooke, J.M., 2013, River Meandering, in Wohl, E. and Schroder, I., eds., Treatise on Geomorphology, Volume 9: San Diego, California, Academic Press, p. 260–288, https://doi.org/10.1016/B978-0-12-374739-6.00241-4.

Seminara, G., 2006, Meanders: Journal of Fluid Mechanics, v. 554, p. 271, https://doi.org/10.1017/S0022112006008925.

Sylvester, Z., Durkin, P., and Covault, J.A., 2019, High curvatures drive river meandering: Geology, v. 47, p. 263–266, https://doi.org/10.1130/G45608.1.

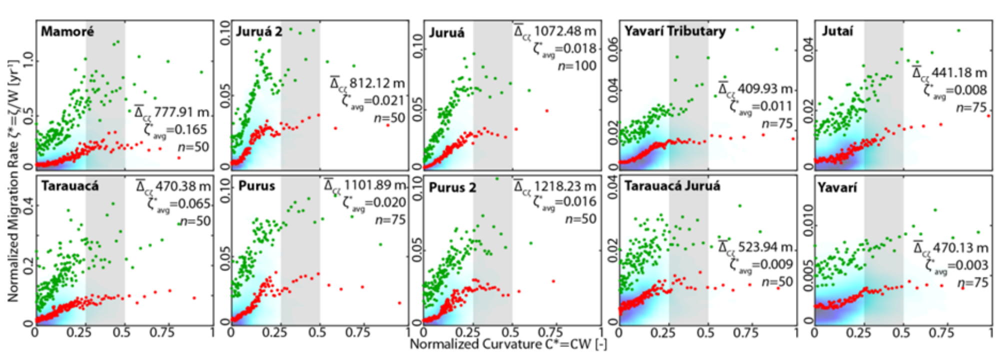

Figure 1. Width-normalized migration rates ($\zeta^* = \zeta/W$), corrected for the reach-averaged lag between maximum migration and curvature ($\overline{\Delta_{\mathcal{C}\zeta}}$), are plotted against the width-normalized curvature ($\mathcal{C}^* = \mathcal{C}W$) for each reach. Red and green dots represent the binned 50th and 95th percentiles of the ζ^* distribution, obtained from a set of n data points specified in each panel. Areas shaded in blue represent the 2-D kernel density estimates of the data. Gray vertical stripes denote the critical $0.25 < \mathcal{C}^* < 0.5$ range. Reach-averaged normalized migration rates (ζ^*_{avg}) decrease from left to right.